Journal of Solid State Chemistry 184 (2011) 1631–1637

Contents lists available at ScienceDirect

Journal of Solid State Chemistry

journal homepage: www.elsevier.com/locate/jssc

Neutron diffraction studies of $RSn_{1+x}Ge_{1-x}$ (R=Tb–Er) compounds

A. Gil [a,*], B. Penc [b], S. Baran [b], A. Hoser [c], A. Szytuła [b]

[a] Department of Mathematics and Natural Sciences, J. Długosz University Częstochowa, Armii Krajowej 13/15, PL 42-200 Częstochowa, Poland
[b] M. Smoluchowski Institute of Physics, Jagiellonian University, Reymonta 4, PL 30-059 Kraków, Poland
[c] BENSC, Helmholtz-Zentrum Berlin, Hahn-Meitner-Platz 1, D 14109 Berlin, Germany

ARTICLE INFO

Article history:
Received 24 February 2011
Received in revised form
23 April 2011
Accepted 24 April 2011
Available online 5 May 2011

Keywords:
Rare-earth intermetallic compound
Magnetic structure
Neutron diffraction

ABSTRACT

The magnetic structures of $RSn_{1+x}Ge_{1-x}$ (R=Tb, Dy, Ho and Er, $x \approx 0.1$) compounds have been determined by neutron diffraction studies on polycrystalline samples. The data recorded in a paramagnetic state confirmed the orthorhombic crystal structure described by the space group *Cmcm*. These compounds are antiferromagnets at low temperatures. The magnetic ordering in $TbSn_{1.12}Ge_{0.88}$ is sine-modulated described by the propagation vector $\mathbf{k}$=(0.4257(2), 0, 0.5880(3)). Tb magnetic moment equals 9.0(1) μ_B at 1.62 K. It lies in the b–c plane and form an angle θ=17.4(2)° with the c-axis. This structure is stable up to the Nèel temperature equal to 31 K. The magnetic structures of $RSn_{1+x}Ge_{1-x}$, where R are Dy, Ho and Er at low temperatures are described by the propagation vector $\mathbf{k}$=(1/2, 1/2, 0) with the sequence (++−+) of magnetic moments in the crystal unit cell. In $DySn_{1.09}Ge_{0.91}$ and $HoSn_{1.1}Ge_{0.9}$ magnetic moments equal 7.25(15) and 8.60(6) μ_B at 1.55 K, respectively. The moments are parallel to the c-axis. For Ho-compound this ordering is stable up to T_N=10.7 K. For $ErSn_{1.08}Ge_{0.92}$, the Er magnetic moment equals 7.76(7) μ_B at T=1.5 K and it is parallel to the b-axis. At T_t=3.5 K it tunes into the modulated structure described by the $\mathbf{k}$=(0.496(1), 0.446(4), 0). With the increase of temperature there is a slow decrease of k_x component and a quick decrease of k_y component. The Er magnetic moment is parallel to the b-axis up to 3.9 K while at 4 K and above it lies in the b–c plane and form an angle 48(3)° with the c-axis. In compounds with R=Tb, Ho and Er the magnetostriction effect at the Nèel temperature is observed.

1. Introduction

The rare-earth (R) ternary intermetallics have been extensively investigated for many years. These compounds exist in different compositions. The magnetic properties depend on distribution of other elements. Up to now the investigations were concentrated on the R–T–X compounds where T is a d-electron element and X is a metalloid. Recently, nearly stoichiometric compounds with general formula $RSn_{1+x}Ge_{1-x}$, where R=Y, Gd–Tm, $x \approx \pm 0.15$, have been reported. These compounds crystallize in the centrosymmetric space group *Cmcm* and they are antiferromagnets with the Nèel temperatures between 29 K for R=Tb and 0.9 K for R=Tm [1]. The crystal structures of these compounds are similar to those in which RT_xX_2 compounds crystallize. The RT_xX_2 compounds are the object of intensive investigations in our group (see Ref. [2] and references there in).

This work reports the results of X-ray and neutron diffraction measurements. The crystal and magnetic structures of $RSn_{1+x}Ge_{1-x}$ (R=Tb–Er; $x \approx 0.1$) have been determined. The aim of the studies was to determine the microscopic properties of these compounds and comparison with the macroscopic data presented in Ref. [1].

The obtained results are also compared with those for RT_xX_2 (X=Ge, Sn) with the purpose to determine the influence of other elements on the magnetic ordering in the rare-earth sublattices.

2. Methods of investigation

Polycrystalline samples of $RSn_{1+x}Ge_{1-x}$ (R=Tb, Dy, Ho, Er, $x \approx 0.1$) were synthesized by arc melting high purity elements (R: 99.9 wt%; Sn and Ge: 99.99 wt%) in a titanium-gettered argon atmosphere. The compositions of the samples are the same as presented in Ref. [1]. Afterwards, the samples were annealed in evacuated quartz ampoules at 773 K for 1 week. The stoichiometry of the samples was controlled by weight before and after the melting. The differences were smaller than 0.5%.

The quality of the samples was checked by X-ray powder diffraction at room temperature on a Philips PW-3710 X'PERT diffractometer using Cu$K\alpha$ radiation. All samples exhibited the orthorhombic *Cmcm* crystal structure. The small impurity of pure

* Corresponding author.
E-mail address: a.gil@ajd.czest.pl (A. Gil).

0022-4596/$ - see front matter © 2011 Elsevier Inc. All rights reserved.
doi:10.1016/j.jssc.2011.04.040

tin, rare-earth oxides and no identified phase in the Tb-compound were observed.

The neutron diffraction patterns were collected at temperatures ranging from 1.45 to 37.6 K on the E6 diffractometer installed at the BER II reactor (BENSC, Helmholtz-Zentrum Berlin). The incident neutron wavelength was 2.447 Å.

For Tb-, Ho- and Er-compounds the measurements in different temperatures were performed with the purpose to determine the temperature dependence of magnetic moments and lattice parameters. For Dy-compound the measurements were performed at 1.55 and 25.5 K only because of the large absorption effect.

The X-ray and neutron diffraction data were analyzed using the Rietveld-type program Fullprof [3]. In the case of $DySn_{1.09}Ge_{0.91}$ the absorption effect was taken into consideration.

3. Results

3.1. Crystal structure

The X-ray diffraction data collected at room temperature as well as the neutron diffraction data recorded in paramagnetic state unambiguously confirms that the investigated compounds crystallize in the orthorhombic crystal structure (space group *Cmcm*, no. 63). In the unit cell all the atoms are located at the 4(*c*) site (0, *y*, 1/4) with different values of the positional parameters y_i for *R*, Sn and Ge atoms. The calculations were performed assuming that the additional Sn atoms ($x>0$) occupy statistically Ge sites. The values of the lattice parameters and free positional parameters y_i determined from the neutron diffraction data in paramagnetic state are listed in Table 1. The obtained parameters are in a good agreement with previous data [1]. Analysis of the neutron diffraction patterns, measured below the Nèel temperatures as a function of temperature, indicates that the crystal structure does not change.

3.2. Magnetic structure

Figs. 1–4 present the neutron diffractograms obtained for the $RSn_{1+x}Ge_{1-x}$ ternaries (*R*=Tb, Dy, Ho and Er, respectively). Comparison of the diffraction patterns taken at low temperatures with those collected in the paramagnetic state clearly reveal the presence of some additional reflections due to the magnetic ordering. In the following, the neutrons diffraction results are discussed separately for each compound. Analyzing positions of additional reflections propagation vectors were determined, while peak intensities analysis allowed to determine the value of the magnetic moments and their directions by the Euler angles θ and φ (relatively to the *c*- and *a*-axis of the orthorhombic cell).

Table 1
Values of the lattice parameters *a*, *b* and *c*, the unit cell volumes *V*, the positional atom parameters y_i, for $RSn_{1+x}Ge_{1-x}$ (*R*=Tb, Dy, Ho and Er) compounds derived from the neutron diffraction data collected at different temperatures in paramagnetic state.

R	$TbSn_{1.12}Ge_{0.88}$	$DySn_{1.09}Ge_{0.91}$	$HoSn_{1.1}Ge_{0.9}$	$ErSn_{1.08}Ge_{0.92}$
T(K)	37.6	25.5	16.2	9.8
a(Å)	4.2541(9)	4.2249(15)	4.2203(7)	4.1921(30)
b(Å)	16.3117(41)	16.2816(49)	16.0901(34)	16.0057(50)
c(Å)	4.0355(10)	4.0111(12)	4.0216(7)	4.0012(8)
V(Å^3)	280.05(20)	275.92(26)	273.09(15)	268.47(67)
y_R	0.0974(6)	0.1043(8)	0.0982(5)	0.090(9)
y_{Sn}	0.7462(7)	0.7555(17)	0.7440(5)	0.7481(9)
y_{Ge}	0.4464(4)	0.4523(13)	0.4449(3)	0.4466(5)
R_{Bragg}(%)	11.9	14.4	10.3	10.4
R_{prof}(%)	9.4	10.1	5.8	8.7

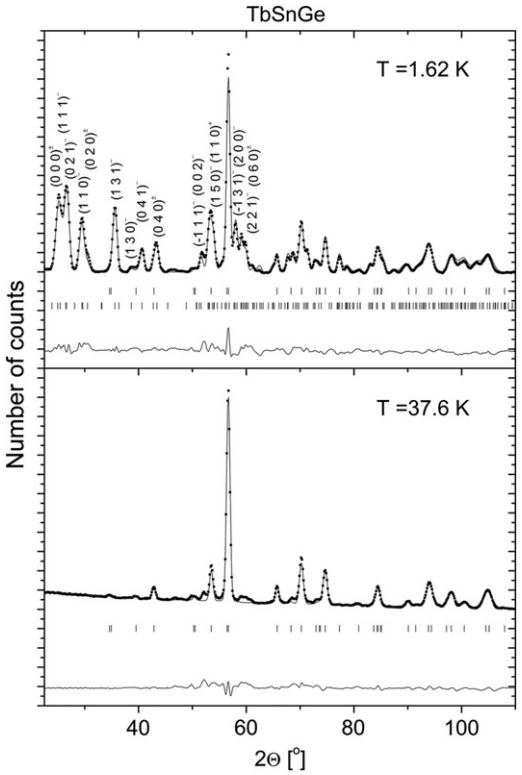

Fig. 1. Neutron diffraction patterns of $TbSn_{1.12}Ge_{0.88}$ collected at 1.62 and 37.6 K. The symbols represent the experimental data, and the solid lines are the calculated profiles for the crystal and magnetic structure models (see the text). The difference between the observed and calculated intensities is shown at the bottom of each diagram. The vertical bars indicate the positions of the Bragg peaks of nuclear (first row) and magnetic (second row) origin. The additional peaks at $2\theta=50^\circ$ and 60° correspond to the no identified impurity phase.

3.2.1. $TbSn_{1.12}Ge_{0.88}$

In the neutron diffraction pattern collected at 1.62 K (Fig. 1) additional peaks of magnetic origin are observed. These peaks are indexed with the propagation vector $\mathbf{k}=(0.4257(2), 0, 0.5880(3))$ which corresponds to an incommensurate magnetic structure. Similar magnetic structures were observed in $DyNi_{0.22}Sn_2$ [4], $DySn_2$ and $ErSn_2$ [5].

The rare-earth moments occupy the following positions in crystal unit cell: μ_1 (0, *y*, 1/4), μ_2 (0, $-y$, 3/4), μ_3 (1/2, 1/2+*y*, 1/4) and μ_4 (1/2, 1/2−*y*, 3/4). The eight models of the moment arrangements in the chemical cell, namely [5]:

1	2	3	4	5	6	7	8
$+\mu_1$	$-\mu_1$	$+\mu_1$	$+\mu_1$	$+\mu_1$	$+\mu_1$	$+\mu_1$	$+\mu_1$
$+\mu_2$	$+\mu_2$	$-\mu_2$	$+\mu_2$	$+\mu_2$	$-\mu_2$	$-\mu_2$	$+\mu_2$
$+\mu_3$	$+\mu_3$	$+\mu_3$	$-\mu_3$	$+\mu_3$	$-\mu_3$	$+\mu_3$	$-\mu_3$
$+\mu_4$	$+\mu_4$	$+\mu_4$	$+\mu_4$	$-\mu_4$	$+\mu_4$	$-\mu_4$	$-\mu_4$

have been tested.

The best fit of the experimental data are obtained for the model in which all Tb magnetic moments in the crystal unit cell are coupled ferromagnetically corresponding to the first model mentioned above. The magnitudes of Tb moments are described

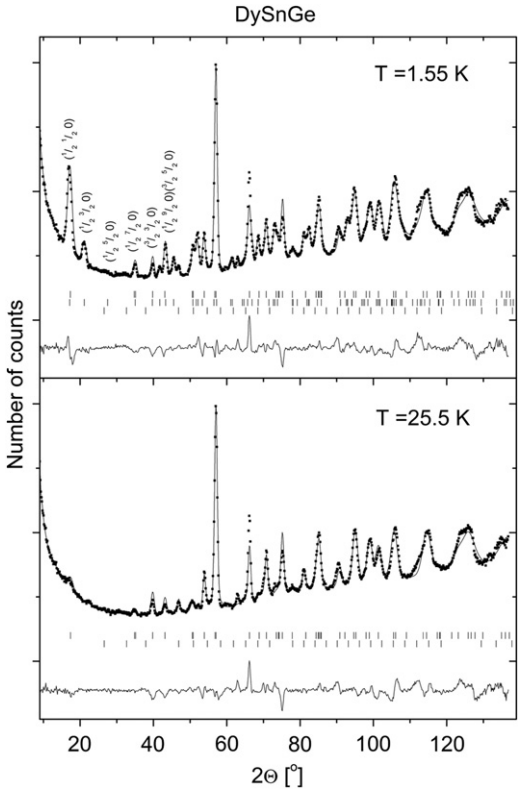

Fig. 2. Neutron diffraction patters of $DySn_{1.09}Ge_{0.91}$ collected at 1.55 and 25.5 K. Description similar as to Fig. 1. The vertical bars indicate the position of the Bragg peaks of nuclear origin (first row) and of Dy_2O_3 impurity (second row) on pattern at 25.5 K and nuclear (first row), magnetic (second row) and impurity (third row) at 1.55 K, respectively. The additional peaks at $2\theta = 47.9^\circ$, 64.7° and 81.9° correspond to the Dy_2O_3.

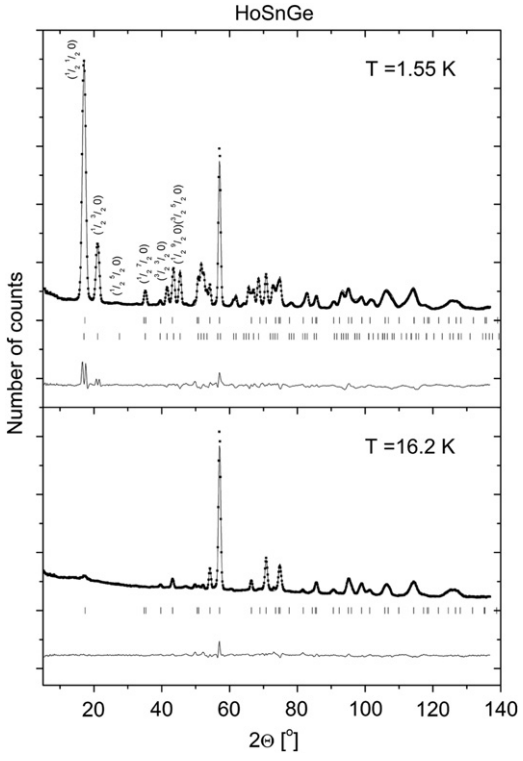

Fig. 3. Neutron diffraction patterns of $HoSn_{1.1}Ge_{0.9}$ collected at 1.55 and 16.2 K. Description similar as to Fig. 1.

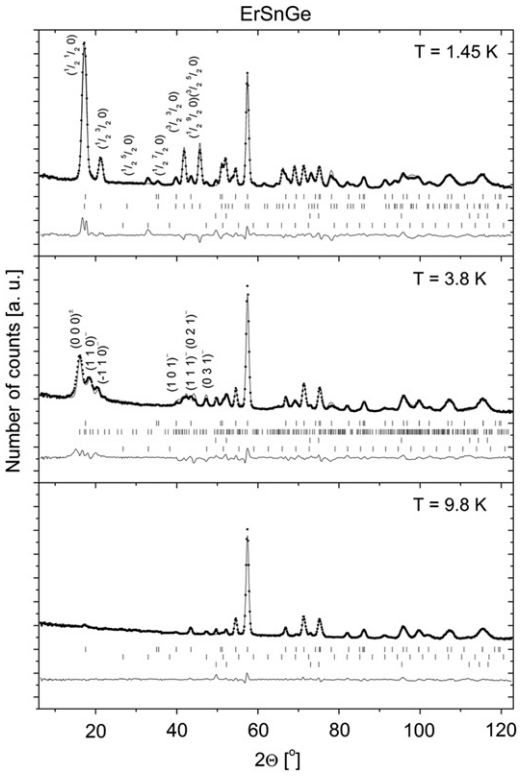

Fig. 4. Neutron diffraction patterns of $ErSn_{1.08}Ge_{0.92}$ collected at 1.45, 3.8 and 9.8 K. Description similar as to Fig. 1. The vertical bars indicate the position of the Bragg peaks of nuclear origin (first row), Er_2O_3 impurity (second row) and Sn (third row) on pattern at 9.8 K. On patterns at 3.8 K and 1.45 K the vertical bars correspond to the nuclear, magnetic and impurities, respectively.

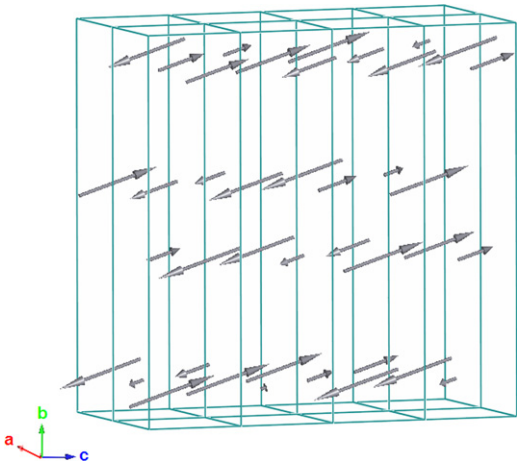

Fig. 5. Magnetic structures of $TbSn_{1.12}Ge_{0.88}$.

by the formula $\mu(\vec{r}) = \mu_0 \sin(\vec{k} \cdot \vec{r} + \phi)$, where μ_0 denotes the amplitude of modulation and **r** is a vector pointing from the beginning of the coordinates systems. The moments lie in the *b*–*c* plane and form an angle $\theta = 17.4(2)^\circ$ with the *c*-axis. They form a sine modulated structure with the amplitude equal to 9.0(1) μ_B ($R_{mag} = 7.5\%$). The magnetic structure of $TbSn_{1.12}Ge_{0.88}$ is presented in Fig. 5. Temperature dependence of the Tb magnetic moment (see Fig. 6) indicates that this type of magnetic ordering is stable up to the Nèel temperature equal to 31 K. The components of the propagation vector k_x increase while k_z decrease with increasing temperature. Temperature dependence of the lattice parameters *a*, *b* and *c* and unit cell volume *V* (see Fig. 7) indicate the small magnetostriction effect at T_N.

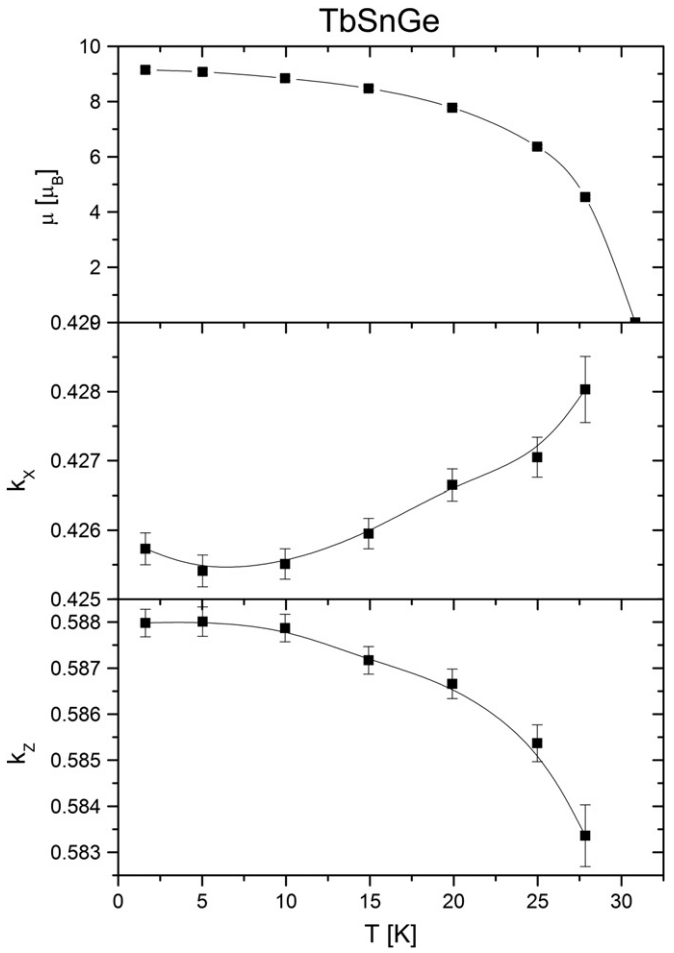

Fig. 6. Temperature dependence of the Tb magnetic moment μ and k_x and k_z components of the propagation vector for $TbSn_{1.12}Ge_{0.88}$.

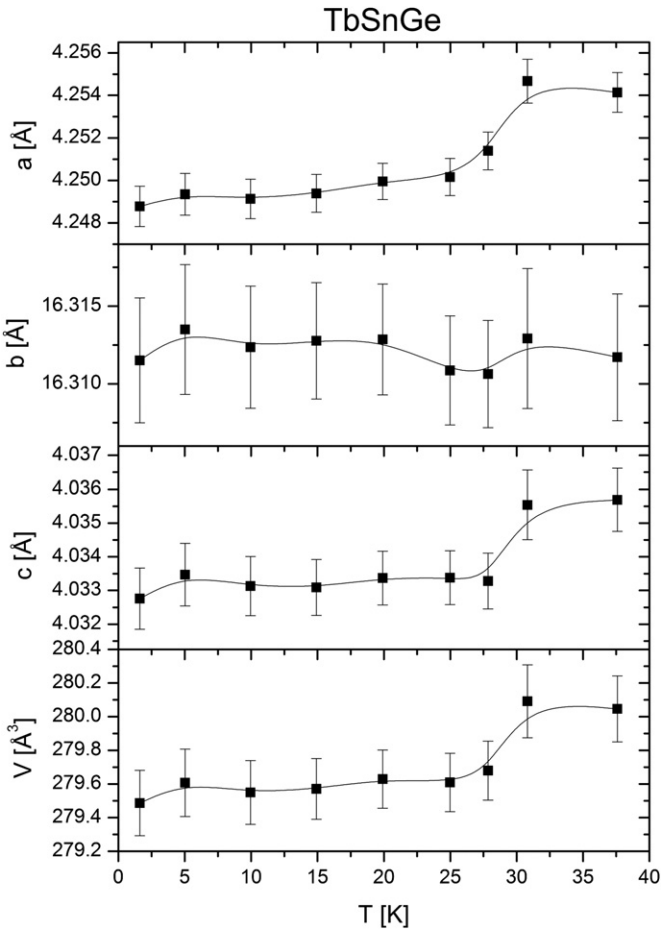

Fig. 7. Temperature dependence of the lattice parameters a, b and c and the unit cell volume V for $TbSn_{1.12}Ge_{0.88}$.

3.2.2. $DySn_{1.09}Ge0.91$

The neutron diffractograms collected for $DySn_{1.09}Ge_{0.91}$ at 1.55 K are displayed in Fig. 2. All additional Bragg peaks of magnetic origin can be well described by the propagation vector $\mathbf{k}=(1/2, 1/2, 0)$. The observed zero intensity of the (1/2, 5/2, 0) peak on the neutron diffraction pattern suggests the following arrangement of the magnetic moments $\mu_1=\mu_2=\mu_4=-\mu_3$ corresponding to the 4th model mentioned above. Such arrangement is in a good agreement with the group theory analysis [6].

The Dy magnetic moments equal 7.25(15) μ_B and they are parallel to the c-axis ($R_{mag}=11.3\%$). The magnetic structure is presented in Fig. 8. The large intensity of the (1/2, 1/2, 0) reflection should be related to the presence of the ferromagnetic (1 1 0) planes. The structure may be viewed as a stacking of ferromagnetic slabs parallel to the (1 1 0) plane. These slabs are antiferromagnetically coupled with the adjacent ones along the stacking direction.

3.2.3. $HoSn_{1.1}Ge_{0.9}$

The neutron diffraction patterns of $HoSn_{1.1}Ge_{0.9}$, below the Nèel temperature (Fig. 3), are similar to those observed for $DySn_{1.09}Ge_{0.91}$ at 1.55 K. This fact indicates similar magnetic ordering described by the propagation vector $\mathbf{k}=(1/2, 1/2\ 0)$. The Ho magnetic moments equal 8.60(6) μ_B and they are parallel to the c-axis ($R_{mag}=8.9\%$). Magnetic structure of $HoSn_{1.1}Ge_{0.9}$ is shown in Fig. 8. This type of magnetic ordering is stable up to the

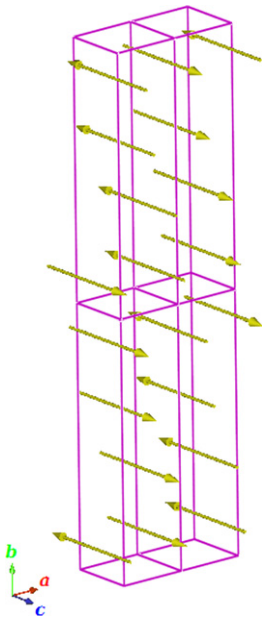

Fig. 8. Magnetic structures of $DySn_{1.09}Ge_{0.91}$ and $HoSn_{1.1}Ge_{0.9}$.

Nèel temperature equal to 10.7 K (see Fig. 9). Temperature dependence of the lattice parameters a, b and c and unit cell volume V (see Fig. 9) indicates the strong magnetostriction at T_N.

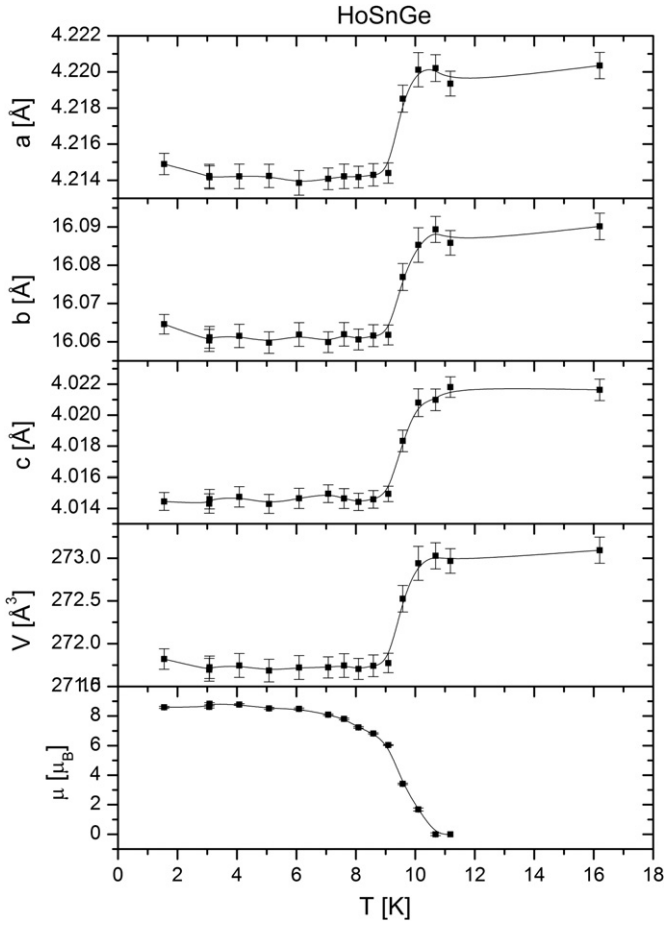

Fig. 9. Temperature dependence of the lattice parameters a, b and c, the unit cell volume V and the value of the magnetic moment μ for $HoSn_{1.1}Ge_{0.9}$.

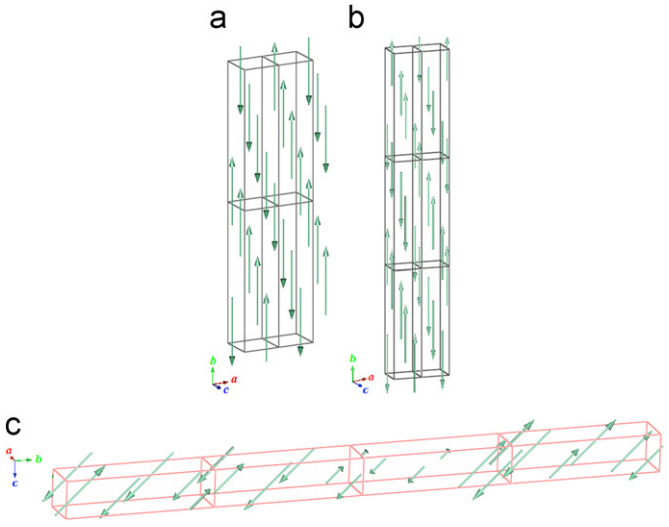

Fig. 10. Magnetic structures of $ErSn_{1.08}Ge_{0.92}$: (a) at low temperatures, (b) near to the phase transition, and (c) close to the Nèel temperature.

3.2.4. $ErSn_{1.08}Ge_{0.92}$

The diffractogram of $ErSn_{1.08}Ge_{0.92}$, taken at 1.45 K (Fig. 4), reveals the presence of additional reflections due to a magnetic ordering similar to those observed for Dy- and Ho-compounds. The magnetic structure is described by the propagation vector $\mathbf{k}=(1/2, 1/2, 0)$. The Er moments equal 7.76(7) μ_B and they are parallel to the b-axis ($R_{mag}=6.8\%$) (see Fig. 10a). This type of magnetic ordering is stable up to 3.5 K. Above this temperature a change of the magnetic structure to a modulated, incommensurate with crystal one, described by the propagation vector $\mathbf{k}=(k_x, k_y, 0)$ is observed. In this temperature range the Er magnetic moments form a sine modulated structure. The magnitude of magnetic moment is described by the formula $\mu(\vec{r})=\mu_0 \sin(\vec{k}\cdot\vec{r})$, where amplitude of modulation is equal to 7.33(16) μ_B at 3.8 K ($R_{mag}=11.5\%$).

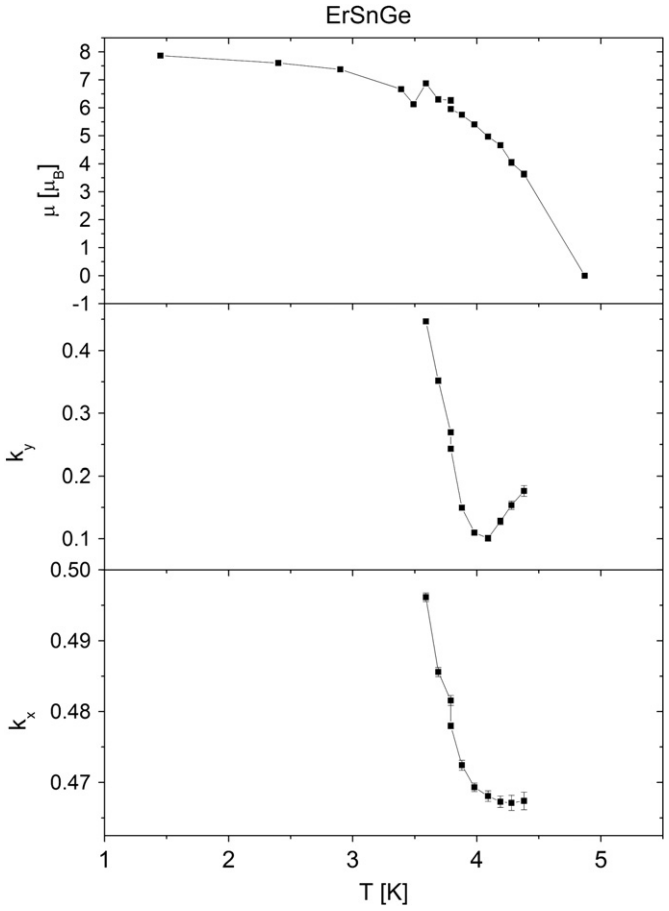

Fig. 11. Temperature dependence of the Er magnetic moment μ and k_x and k_y components of the propagation vector for $ErSn_{1.08}Ge_{0.92}$.

Fig. 11 presents the temperature dependences of the Er magnetic moment and k_x, k_y components of the propagation vector. Temperature dependence of the Er magnetic moment shows a small anomaly at $T_t=3.5$ K and the Nèel temperature equals 4.9 K. Above T_t both components of the propagation vector decrease, particularly k_y shows anomalous behavior close to the Nèel temperature. The magnetic moment is parallel to the b-axis up to 3.9 K (Fig. 10b) while at 4 K and above it lies in the b–c plane and form an angle 48(3)° with the c-axis (Fig. 10c).

The temperature dependence of the lattice parameters a, b and c and the unit cell volume V (see Fig. 12) clearly indicates strong magnetostriction effect at the Nèel temperature T_N and a small one at T_t.

4. Discussion

The results for $RSn_{1+x}Ge_{1-x}$ (R=Tb–Er) series presented in this work confirm the orthorhombic structure described by the space group *Cmcm* (no. 63) similar to that proposed in Ref. [1]. The determined positional parameters for all compounds are in

good agreement with those obtained from the X-ray single crystal data for TmSnGe [1].

The investigated compounds are antiferromagnets at low temperatures. The values of the respective Nèel temperatures for Tb-, Ho- and Er-compounds, determined by means of the neutron diffraction studies, are in a good agreement with previously published ones based on the magnetic and specific heat data [1]. On the basis of the neutron diffraction data the magnetic structures of these compounds were determined. For Dy-, Ho- and Er compounds the magnetic ordering at low temperatures near 1.5 K is described by the propagation vector $\mathbf{k}=(1/2, 1/2, 0)$. For $HoSn_{1.1}Ge_{0.9}$ compound this ordering is stable up to the Nèel temperature equal to 10.7 K, while for $ErSn_{1.08}Ge_{0.92}$ with increase of temperature the change of the magnetic structure to a modulated, incommensurate with the crystal one is observed.

The magnetic structure of $TbSn_{1.12}Ge_{0.88}$ is different to those observed in other $RSn_{1+x}Ge_{1-x}$ compounds and in $TbSn_2$ [5]. The latter compound has a collinear antiferromagnetic structure described by the propagation vector $\mathbf{k}=(0, 0, 1/2)$.

Crystal structures of $RSn_{1+x}Ge_{1-x}$ compounds are similar to those observed in RT_xX_2 compounds. Both groups of compounds crystallize in the orthorhombic structure described by the space group *Cmcm* (no. 63). In both groups the atoms *R*, Sn, Ge in the first and *R*, *T*, *X* in the second group are located in alternating layers stacked along the *b*-axis with the following sequence Ge–*R*–Sn–*R*–Sn–*R* for $RSn_{1+x}Ge_{1-x}$ and *X*–*R*–*T*–*X*–*T*–*X*–*R* for RT_xX_2.

The magnetic data for RT_xX_2 compounds indicate that, except for *T*=Mn, the *T* atoms with 3*d*-electrons do not have a localized magnetic moment. This fact suggests that in both groups of compounds the magnetic moment localized on the rare-earth atoms form an antiferromagnetic ordering.

Table 2 summarizes the magnetic structure types in the investigated $RSn_{1+x}Ge_{1-x}$ and RT_xSn_2 and RT_xGe_2 (*R*=Tb–Er; *T*=Cr, Fe, Co, Ni) families. Except five types proposed for stannides in Ref. [5] five additional types described by magnetic ordering in investigated compounds and germanides are added.

In $RSn_{1+x}Ge_{1-x}$ compounds with *R*=Dy, Ho and Er magnetic ordering in temperatures close to 1.5 K is described by the propagation vector $\mathbf{k}=(1/2, 1/2, 0)$. The magnetic ordering with this propagation vector is observed in a large number of Ho-germanides and stannides; for example in germanides with *T*=Cr [2], Fe [4], Co [7] and stannides $HoSn_2$ [5] likewise in those with *T*=Fe [8], Co [9] and Ni [10]. Such as in these compounds so in $HoSn_{1.1}Ge_{0.9}$ this magnetic ordering is stable up to the Nèel temperature. Interesting results are observed in $ErSn_{1.08}Ge_{0.92}$ compound where the change of the magnetic structure from collinear commensurate with the crystal one at low temperatures to the modulated incommensurate above the Nèel temperature is observed. This is clearly visible in the presented neutron diffraction data. The specific heat data (see Fig. 3 in Ref. [1]) give only widening of the maximum near the Nèel temperature.

In the investigated $RSn_{1+x}Ge_{1-x}$ and RT_xX_2 compounds the large *R*–*R* interatomic distances, about 4 Å in the *b*–*c* plane and 3.5 Å along the *b*-axis, and metallic character of the electrical resistivity [1] indicate that the magnetic ordering in the rare-earth sublattice is realized by the magnetic interactions with the conduction electrons (*R*KKY interaction). In this type of interaction the Nèel temperatures should be proportional to the de Gennes factor $(g_J-1)^2J(J+1)$. For $RSn_{1+x}Ge_{1-x}$ compounds this relation is fulfilled for *R*=Tb–Tm (see Fig. 5 in Ref [1]). The *R*KKY interactions are long-range and this should lead in general, to modulated magnetic structures. The determined magnetic structures have such character. With increase of temperature the change of magnetic structure in $ErSn_{1.08}Ge_{0.92}$ from the collinear commensurate to the modulated incommensurate is observed. Such change is quite common among rare earth intermetallics and may be explained as a result of a competition between different types of interactions [11].

Another factor which affects the magnetic ordering in the intermetallic compounds is the crystal electric field (CEF) effect which determines the direction of a magnetic moment. In the

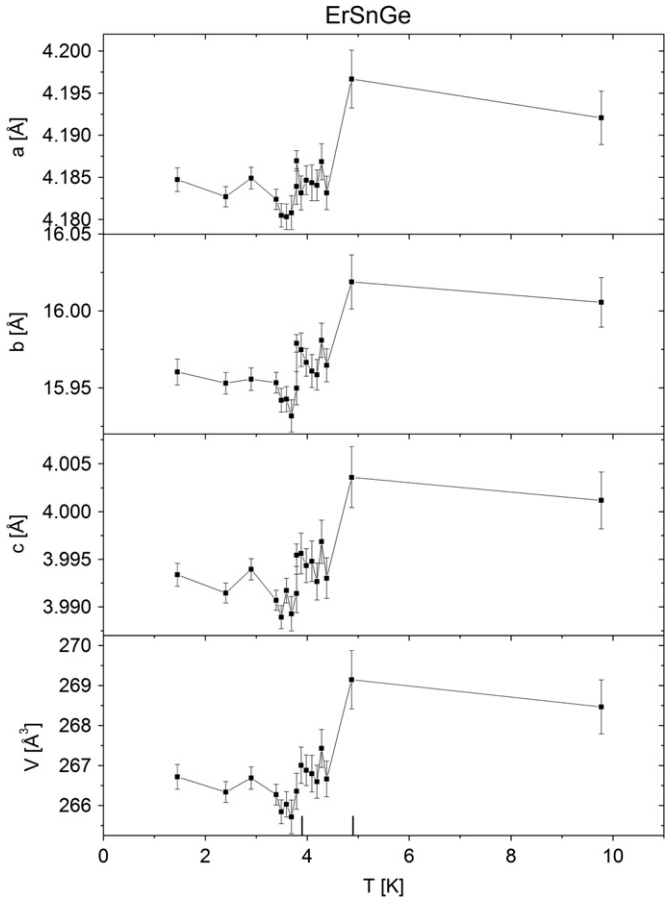

Fig. 12. Temperature dependence of the lattice parameters *a*, *b*, *c* and unit cell volume *V* for $ErSn_{1.08}Ge_{0.92}$.

Table 2
Comparison of the magnetic structures of $RSn_{1+x}Ge_{1-x}$ compounds and structures of RSn_2, RT_xSn_2 and RT_xGe_2.

R	$RSn_{1+x}Ge_{1-x}$	RSn_2	RFe_xSn_2	RCo_xSn_2	RNi_xSn_2	RCr_xGe_2	RFe_xGe_2	RCo_xGe_2	RNi_xGe_2	RCu_xGe_2
Tb	SM1	AF1→SM1	AF1	AF1	AF1	AF4	–	–	AF6	AF6
Dy	AF2	AF3→SM1	AF1	–	SM1	AF4→AF5	–	–	–	–
Ho	AF2	AF2→SM1	AF2	AF2	AF2	AF2	AF2	AF2	AF6	AF6
Er	AF2→SM4	AF1→SM1	AF2	AF1	AF1	SM3	SM2	SM4	AF6	AF6

AF—antiferromagnetic structure; SM—sine modulated structure.
The marks according to Ref. [5]: AF1—$\mathbf{k}=(0, 0, 1/2)$; AF2—$\mathbf{k}=(1/2, 1/2, 0)$; AF3—$\mathbf{k}=(1/2, 1/2, 1/2)$; AF4 (new)—$\mathbf{k}=(1/2, 0, 0)$; AF5 (new)—$\mathbf{k}=(1/2, 0, 1/2)$; AF6 (new)—$\mathbf{k}=(0, 0, 0)$; SM1—$\mathbf{k}=(k_x, 0, k_z)$; SM2—$\mathbf{k}=(0, k_y, k_z)$; SM3 (new) $\mathbf{k}=(0, 0, k_z)$; SM4—$\mathbf{k}=(k_x, k_y, 0)$ (new)—see text.

investigated $RSn_{1+x}Ge_{1-x}$ compounds for R=Tb, Dy and Ho the magnetic moments are smaller than for free R^{3+} ion values. This indicates the influence of the crystal electric field. The orientation of the rare-earth magnetic moments also confirms the influence of the CEF effect. In $TbSn_{1.12}Ge_{0.88}$ the Tb magnetic moment form an angle 17.4(2)° with the c-axis. In Dy- and Ho-compounds the rare-earth magnetic moments are parallel to the c-axis. At low temperatures the Er magnetic moment in $ErSn_{1.08}Ge_{0.92}$ is parallel to the b-axis while close to the Nèel temperature the orientation of the magnetic moment changes, it lies in the b–c plane and form an angle 48(3)° with the c-axis.

The rare-earth site in these compounds has a point symmetry mm. The CEF Hamiltonian is

$$H_{CF} = B_2^0O_2^0 + B_2^2O_2^2 + B_4^0O_4^0 + B_4^2O_4^2 + B_4^4O_4^4 + B_6^0O_6^0 + B_6^2O_6^2 + B_6^4O_6^4 + B_6^6O_6^6$$

where B_n^m are CEF parameters and O_n^m are the Stevens operator [12]. The orientation of the magnetic moment is determined by the sign of B_2^0 parameter [13]. When the magnetic moment is parallel to the c-axis B_2^0 is negative. The positive value of B_2^0 stabilizes the other magnetic moment direction.

The crystal field parameters B_n^m can be written as

$$B_n^m = A_n^m \langle r^n \rangle \theta_n$$

where A_n^m is the crystal field coefficient which characterizes the surrounding charge distribution, $\langle r^n \rangle$ is the mean value of the nth power of the 4f radius and θ_n is the appropriate Stevens factor [14].

The observed change in orientation of the rare-earth magnetic moments between Ho- and Er-compounds is due to change of the Stevens factor α_J sign from negative for Ho to positive for Er.

The deviations from the c-axis of the magnetic moment in $TbSn_{1.12}Ge_{0.88}$ and from the b-axis in $ErSn_{1.08}Ge_{0.92}$ near the Nèel temperature suggest the influence of higher order CEF parameters.

5. Summary

The results presented in this work indicate that the magnetic ordering in $RSn_{1+x}Ge_{1-x}$ compounds is similar to those observed in RT_xX_2 compounds. The Nèel temperatures for both series of compounds are also similar. The neutron diffraction data indicates that the magnetic moment is localized on the rare-earth atoms. The large R–R interatomic distances and metallic character of the electrical resistivity suggest that interaction between magnetic moments takes place via conduction electrons. Comparing the magnetic properties for both groups of compounds it can be inferred that other elements (T, Sn, Ge) have not got significant influence on stability of the magnetic ordering.

Acknowledgments

The work was supported by the European Commission under the 7th Framework Program through the key Action: Strengthening the European Research Area, Research Infrastructures, Contract no. RI-CP-2008-226507 (NMI3-II).

References

[1] P.H. Tobash, J.J. Meyers, G. DiFilippo, S. Bobev, F. Ronning, J.D. Thompson, J.L. Sarrao, Chem. Mater. 20 (2008) 2151–2159.
[2] A. Gil, D. Kaczorowski, B. Penc, A. Hoser, A. Szytuła, J. Solid State Chem. 184 (2011) 227–235.
[3] J. Rodriguez-Carvajal, Physica B 192 (1993) 55–69.
[4] A. Gil, B. Penc, J. Hernandez-Velasco, A. Szytuła, A. Zygmunt, Phys. B: Condens. Matter 355 (2004) L1–L3.
[5] G. Venturini, P. Lemoine, B. Malaman, B. Ouladdiat, J. Alloys Compd. 505 (2010) 404–415.
[6] S. Baran, Ł. Gondek, J. Hernandez-Velasco, D. Kaczorowski, A. Szytuła, J. Magn. Magn. Mater. 285 (2005) 188–192.
[7] S. Baran, F. Henkel, D. Kaczorowski, J. Hernandez-Velasco, B. Penc, N. Stüsser, A. Szytuła, E. Wawrzyńska, J. Alloys Compd. 415 (2006) 1–7.
[8] B. Malaman, G. Venturini, J. Alloys Compd. 494 (2010) 44–51.
[9] A. Gil, B. Penc, E. Wawrzyńska, J. Hernandez-Velasco, A. Szytuła, A. Zygmunt, J. Alloys Compd. 365 (2004) 31–34.
[10] A. Gil, B. Penc, S. Baran, J. Hernandez-Velasco, A. Szytuła, A. Zygmunt, J. Alloys Compd. 361 (2003) 32–35.
[11] D. Gignoux, D. Schmitt, Phys. Rev. B 48 (1993) 12682–12691.
[12] N.T. Hutchings, Solid State Phys. 16 (1964) 227–273.
[13] A. Szytuła, in: K.H.J. Buschow (Ed.), Handbook of Magnetic Materials, vol. 6, Elsevier Sciences Publ. B.V, 1991, p. 85.
[14] K.W.H. Stevens, Proc. Phys. Soc. A65 (1952) 209.